Phenylpropanoids and Flavonoids from *Phlomis kurdica* as Inhibitors of Human Lactate Dehydrogenase

Ammar Bader [a], Tiziano Tuccinardi [b,c], Carlotta Granchi [b], Adriano Martinelli [b,c], Marco Macchia [b,c], Filippo Minutolo [b,c], Nunziatina De Tommasi [d,*], Alessandra Braca [b,c]

[a] *Department of Pharmacognosy, Faculty of Pharmacy, Umm Al-Qura University, P.O. Box 13174, 21955 Makkah, Saudi Arabia*

[b] *Dipartimento di Farmacia, Università di Pisa, via Bonanno 6 and 33, 56126 Pisa, Italy*

[c] *Centro Interdipartimentale di Ricerca "Nutraceutica e Alimentazione per la Salute", Università di Pisa, via del Borghetto 80, 56124 Pisa, Italy*

[d] *Dipartimento di Farmacia, Università degli Studi di Salerno, via Giovanni Paolo II 132, 84084 Fisciano (SA), Italy*

* Corresponding author. Tel.: +39-089-969754; fax: +39-089-969602.

E-mail address: detommasi@unisa.it (N. De Tommasi).

Abstract

Two new flavonoids, jaceosidin 7-*O*-β-D-glucopyranosyl-(1→2)-β-D-glucopyranoside (**1**) and hispidulin 7-*O*-β-D-glucopyranosyl-(1→2)-β-D-glucopyranoside (**2**), and one new phenylpropanoid, 3,3'-dimethyl-lunariifolioside (**3**), along with 11 known compounds (**4**-**14**), were isolated from the aerial parts of *Phlomis kurdica* growing in Jordan. Structures of **1**-**3** were elucidated on the basis of spectroscopic data. These isolated compounds were assayed for their inhibitory activity against isoform 5 of human lactate dehydrogenase. Compound **4**, luteolin 7-*O*-β-D-glucopyranoside, showed an IC_{50} value comparable to that of galloflavin, used as reference compound. Docking studies were carried out to hypothesize the interaction mode of compound **4** in the enzyme active site.

Keywords: Phlomis kurdica; Lamiaceae; LDH inhibitors; flavonoids; phenolics

1. Introduction

Phlomis genus (Lamiaceae family) comprises more than 100 species mainly distributed in the Mediterranean region, central Asia, and China (Limem-Ben Amor et al., 2009). Ten *Phlomis* species are found in the flora of Jordan, which is considered one of most attractive countries in the Middle East due to its biodiversity (Dal Piaz et al., 2009; Malafronte et al., 2012). Among them, *Phlomis kurdica* Rech.f. is a herb up to 60 cm with leaves ± densely (often whitish) stellate-lanate-tomentose, especially below, oblong-ovate, obtuse, cordate at base, crenate, 5-12 x 38 cm, petiole to 11 cm; the yellow flowers arranged in verticillasters 3-6, lower remote, 8-10-flowered (Al-Eisawi, 1998). Many species of *Phlomis* have been used for decades in folk medicine as pain relievers, tonics, wound healers and stimulants (Limem-Ben Amor et al., 2009). Their flowered parts are generally used as herbal tea to treat gastrointestinal disorders and to protect the liver, kidneys, bones and the cardiovascular system (Limem-Ben Amor et al., 2009; Li et al., 2010). Iridoids, flavonoids, phenylpropanoids, phenylethanoids, lignans, neolignans, diterpenoids, alkaloids, and essential oils are typical metabolites of the *Phlomis* genus (Li et al., 2010). Among phenylethanoids, forsythoside B, verbascoside, alyssonoside, and leucosceptosides A and B, have been identified from *P. kurdica* (Kirmizibekmez et al., 2005).

Since extracts of *Phlomis* species showed antiproliferative activity, the crude polar residues of *P. kurdica* aerial parts were assayed for their lactate dehydrogenase (LDH) inhibitory activity, an enzyme whose isoform 5 (*h*LDH5) is up-regulated in human tumor tissues (Granchi and Minutolo, 2012). In fact, cancer cells depend mainly on anaerobic respiration and their glycolytic rate is up to 200 times higher than that of the normal tissue. This fermentative glycolysis is promoted by an overexpression of several enzymes and transporters, which may offer rather safe therapeutic windows for anticancer agents that target them (Granchi and Minutolo, 2012). In particular, the A-subunit of LDH (LDH-A), which exclusively generates *h*LDH5 in its fully functional tetrameric form, catalyzes a crucial step in glycolysis, the reduction of pyruvate to lactate. Therefore,

inhibition of LDH may be considered a promising strategy in cancer treatment, since it should cause a starvation of cancerous cells by reducing their conversion of glucose to lactate (Fiume et al., 2014). So far, several small molecules displaying efficient LDH inhibitory potencies have been reported, and they are generally characterized by the presence of carboxylates and/or phenolic OH groups in their structures (Granchi et al., 2013). These observations prompted the present investigation of *P. kurdica* aerial parts. Hence, two new flavonoids (**1**-**2**) and one new phenylethanoid (**3**), together with eleven known phenolic compounds (**4**-**14**) (Fig.1), including flavonoids and phenylethanoids, were isolated and assayed for their LDH inhibitory activity.

2. Results and discussion

During a wide screening for LDH inhibitory activity, the $CHCl_3$-MeOH, the MeOH and the *n*-BuOH extracts of *P. kurdica* aerial parts were assayed. The $CHCl_3$-MeOH and the *n*-BuOH extracts showed a promising inhibitory activity and therefore were subjected to different chromatographies to afford three new (**1**-**3**) and 11 known compounds (**4**-**14**).

Compound **1**, a yellow amorphous solid, showed a quasimolecular ion peak at *m/z* 653.1725 for $[M–H]^-$ in the HRESIMS; this result, together with ^{13}C NMR, allowed the assignment of molecular formula $C_{29}H_{34}O_{17}$ to **1**. In the ESIMS spectrum fragments at *m/z* 491 $[M–H–162]^-$ and 329 $[M–H–162–162]^-$ revealed the presence of two hexose residues in the molecule. The UV spectrum of **1** showed two absorption maxima at 340 and 277 nm, indicating its flavone skeleton. Compound **1** aglycone was deduced to be jaceosidin (Martinez et al., 1987) on the basis of the following observation in its ^1H NMR spectrum (Table 1): a 5,6,7-trisubstituted pattern for ring A (one singlet at δ 7.04, one methoxy group at δ 3.93) and a 3',4'-disubstitution for ring B (ABX system signals at δ 6.96, d, J = 8.0 Hz; 7.58, d, J = 2.0 Hz; 7.60, dd, J = 8.0, 2.0 Hz; one methoxy signal at δ 4.00). Two anomeric protons arising from the sugar moieties appeared at δ 4.85 and 5.38 each (d, J = 7.5

Hz), which correlated respectively with signals at δ 104.0 and 99.4 ppm in the HSQC spectrum. Assignments of compound **1** NMR chemical shifts were accomplished by 1D-TOCSY, DQF-COSY, HSQC, and HMBC experiments. DQF-COSY and 1D-TOCSY experiments led to the identification of the sugars as two β-glucopyranosyl units. Hydrolysis of **1** with 1 N HCl followed by GC analysis through a chiral column of the monosaccharides treated with 1-(trimethylsilyl)imidazole in pyridine, led to the assignment of sugar configuration. Key correlation peaks were observed in the HMBC experiment between δ 3.93 (OMe at C-6) and 134.2 (C-6), δ 4.00 (OMe at C-3') and 149.3 (C-3'), δ 5.38 (H-1_{glcI}) and 158.0 (C-7), δ 4.85 (H-1_{glcII}) and 82.0 (C-2_{glcI}). In the light of these data, the structure of **1** was elucidated as 3',6-dimethoxy-4',5,7-trihydroxyflavone 7-*O*-β-D-glucopyranosyl-(1→2)-β-D-glucopyranoside or jaceosidin 7-*O*-β-D-glucopyranosyl-(1→2)-β-D-glucopyranoside.

The molecular formula of compound **2** ($C_{28}H_{32}O_{16}$) was determined by its HRESIMS ($[M - H]^-$ ion at *m/z* 623.1608) and by ^{13}C NMR data. The negative-ion ESIMS showed a major peak at *m/z* 623 $[M–H]^-$ and a fragment at *m/z* 299 $[M–H–162–162]^-$. Comparison of the NMR spectroscopic data of **2** with those of **1** (Table 1) showed that these compounds differ in the B-ring of their flavonoid skeletons. NMR data strongly suggested a 4′-hydroxylation pattern for ring B in **2** (AA'XX' system signals at δ 6.95, d, J_{AX} = 8.5 Hz; 7.91, d, J_{AX} = 8.5 Hz), instead of a 3',4'-dihydroxylation pattern as in **1**, allowing the aglycone to be recognized as hispidulin (Merfort and Wendisch, 1987; Merfort, 1988). Hence, compound **2** was elucidated as 6-methoxy-4',5,7-trihydroxyflavone 7-*O*-β-D-glucopyranosyl-(1→2)-β-D-glucopyranoside or hispidulin 7-*O*-β-D-glucopyranosyl-(1→2)-β-D-glucopyranoside.

The molecular formula of compound **3** was determined as $C_{41}H_{56}O_{23}$ by HRESIMS (*m/z* 915.3120 $[M–H]^-$) and ^{13}C NMR analysis. Its ESIMS data showed a quasimolecular ion peak at *m/z* 915 $[M–H]^-$ and 939 $[M+Na]^+$. Three main fragments at *m/z* 807 $[M+Na–132]^+$, 675 $[M+Na–132–132]^+$, and 661 $[M+Na–132–146]^+$, due to the subsequent loss of two pentose and/or one pentose and one

deoxyhexose moiety, were also observed. The analysis of ^{13}C NMR spectrum (Experimental Section) allowed to allocate 9 signals to the aglycone moiety and 22 to a sugar residue consisting of two hexoses and two pentoses. The ^{1}H NMR spectrum (Experimental Section) of **3** displayed proton signals that are characteristic of a *E*-feruloyl group [three aromatic protons resonating at δ 6.80 (1H, d, J = 8.0 Hz), 7.09 (1H, dd, J = 8.0, 2.0 Hz), 7.21 (1H, d, J = 2.0 Hz) as an ABX system, one methoxy group at δ 3.96 (3H, s) and two *trans* olefinic protons as an AB system at δ 6.39, 7.65 (1H, d, J = 16.0 Hz)] and a 3-methoxy-4-hydroxyphenylethyl moiety [three aromatic protons at δ 6.70 (1H, d, J = 2.0 Hz), 6.72 (1H, dd, J = 8.0, 2.0 Hz), 6.87 (1H, d, J = 8.0 Hz) as an ABX system, one methoxy group at δ 3.79 (3H, s), and an A_2B_2 system assigned to a hydroxyethyl group at δ 2.86 (2H, m), 3.77 (1H, m), 4.06 (1H, m)] (Miyase et al., 1982). Additionally, four anomeric proton resonances appeared at δ 4.36 (1H, J = 7.8 Hz, H-1_{glc}), 5.15 (1H, J = 3.0 Hz, H-1_{apiI}), 5.17 (1H, J = 1.8 Hz, H-1_{rha}), and 4.88 (1H, J = 3.0 Hz, H-1_{apiII}), thus suggesting a tetraglycosidic structure, which is consistent, with the help of the ^{13}C NMR spectrum, with the following C-1 configuration: β for glucose, α for rhamnose, and β for the two apioses. These findings were in accordance with HSQC/^{13}C NMR data, where four corresponding anomeric carbons resonated at δ 104.2, 111.8, 102.9, and 111.0, respectively. 1D-TOCSY, DQF-COSY, HSQC, and HMBC experiments allowed the assignments of compound **3** ^{1}H and ^{13}C NMR signals. The HMBC experiment indicated correlations between δ 5.17 (H-1_{rha}) and 81.5 (C-3_{glc}), 5.15 (H-1_{apiI}) and 68.4 (C-6_{glc}), 4.88 (H-1_{apiII}) and 80.3 (C-4_{rha}), suggesting the proper substitution sites of the sugar moieties. The acylation site was on C-4 of glucose as evidenced by the strong deshielding of H-4_{glc} at δ 4.90. Hydrolysis of **3** with 1N HCl, followed by GC analysis through a chiral column of the trimethylsilylated monosaccharides, permit the assignment of sugars configuration. Hence, compound **3** was characterized as β-(3-methoxy-4-hydroxyphenyl)ethyl-*O*-β-D-apiofuranosyl-(1→6)-*O*-[*O*-β-D-apiofuranosyl-(1→4)-α-L-rhamnopyranosyl-(1→3)]-4-*O*-(*E*)-feruloyl-β-D-

glucopyranoside or 3,3'-dimethyl-lunariifolioside (Calis and Kirmizibekmez, 2004), a new phenylethanoid glycoside.

Eleven known compounds, luteolin 7-*O*-β-D-glucopyranoside (**4**) (Agrawal, 1989), jaceosidin 7-*O*-β-D-glucopyranoside or jaceoside (**5**) (Merfort, 1988), luteolin 7-*O*-sophoroside (**6**) (Imperato and Nazzaro, 1996), hispidulin 7-*O*-β-D-glucopyranoside (**7**) (Merfort and Wendish, 1987), forsythoside B (**8**) (Endo et al., 1982), nepetin 7-*O*-β-D-glucopyranoside (**9**) (Merfort, 1988), luteolin 7-*O*-(6'''-acetyl)-β-D-glucopyranosyl-(1→2)-β-D-glucopyranoside or linariifolioside (**10**) (Ma et al., 1991), leucosceptoside B (**11**) (Miyase et al., 1982), vanillic acid 4-*O*-β-D-glucopyranoside (**12**) (Sakushima et al., 1995), verbascoside (**13**) (Liu et al., 1998), and chlorogenic acid (**14**) (Iwai et al., 2004) were identified by analysis of their spectroscopic data and comparison with literature values.

Plant extracts were assayed on the *h*LDH5 purified isoform to determine their inhibition potencies. The IC_{50} values of chloroform-methanol, methanol, *n*-butanol extracts and isolated compounds from *P. kurdica* are reported in Table 2. All the extracts showed a certain LDH inhibition activity, with IC_{50} values ranging from 0.28 to 0.49 mg/mL. Some of the isolated compounds (**4**-**6**) also showed a promising activity. In particular, compound **4**, luteolin 7-*O*-β-D-glucoside, showed an IC_{50} value of 139.2 μM, which is quite comparable to that of reference phenolic compound galloflavin (Manerba et al., 2012). In order to better characterize its biochemical activity, the most promising compound (**4**) was also subjected to enzymatic assays on *h*LDH1 (LDH-B_4) and the results showed that the compound was not selective, since the IC_{50} value was comparable to that obtained on *h*LDH5 (IC_{50} = 110.0 ± 19.9 μM). From our biochemical evaluations, compound **4** proved to be a potentially interesting LDH inhibitor, although it lacks isoform selectivity. In order to provide a more detailed characterization of its biological properties, the mixed-model inhibition fit to the second order polynomial regression analysis of the rate of conversion of NADH to NAD^+ was applied for obtaining K_i values in the NADH-competition

experiments (Copeland, 2000). These analyses afforded an apparent Michaelis–Menten constant (K_M) of 18 μM and a K_i value of 68 μM which is consistent with the IC_{50} value reported in Table 2. As shown in Fig. 2A, the corresponding Lineweaver-Burk plot clearly highlighted a competitive behavior with respect to NADH. Then, in order to investigate a possible competition between compound **4** and pyruvate (PYR), the same kinetic analysis was repeated in PYR-competition experiments. The results revealed a K_M of 146 μM, a K_i value of 137 μM and the corresponding Lineweaver-Burk plot indicated a non-competitive behavior with respect to PYR (see Fig. 2B). With regards to galloflavin, Manerba et al. reported a *h*LDH5 K_i value for NADH- and PYR-competition of 56.0 and 5.46 μM, respectively (Manerba et al., 2012). The most accurate way to get information on the inhibitor–enzyme binding mode is undoubtedly by means of X-ray crystallographic studies of the corresponding complexes. However, in the absence of these important experimental evidences, theoretical approaches have been widely accepted as secondary tools to produce reliable results (Tuccinardi, 2009). With this aim, molecular modeling studies were carried out in order to better characterize the way this molecule interacts with *h*LDH5. Compound **4** was docked into *h*LDH5 (4M49 PDB code) using GOLD software and the best ranked solution was subjected to 5 ns of molecular dynamic simulation (Verdonk et al., 2003). Fig. 3 displays the hypothetical binding mode of **4** into *h*LDH5. The ligand partially fills the cavity occupied by the nicotinamide riboside portion of NADH (see Fig. 3A) and it is stabilized by a large number of H-bonds and lipophilic interactions with the protein. The aromatic portion of the 3,4-dihydroxyphenyl group shows lipophilic interactions with V136, L165 and I252 and establishes two H-bonds with the nitrogen backbone of S137 and the hydroxyl group of S161 (see Fig. 3B). The 5-hydroxy-4*H*-chromen-4-one forms two H-bonds with the nitrogen backbone of T248 and the hydroxyl group of S249 and shows lipophilic interactions with V31. With regard to the glucoside portion of the ligand, as shown in Fig. 3B, it forms 4 additional H-bonds with the backbone of T95, A96, A98 and N138.

An analysis of the inhibitory properties of these compounds seems to indicate as pharmacophoric portions both the catechol and the monosaccharide moieties. In fact, the most potent inhibitor is

compound **4**, which possesses both of these structural motifs. The docking analysis shows that the catechol portion is fundamental in order to form the two highly energetic H-bonds with the N-H backbone of S137 and the OH of S161. Furthermore, the monosaccharide unit of **4** forms four H-bonds with the backbone protein of residues T95, A96, A98 and N138, which would not be possible in the case of its disaccharide-substituted analogues, since they would not fit properly in that pocket. Actually, also compound **9** displays the same pharmacophoric features of **4** (catechol and monosaccharide substituents), but it possesses an additional methoxy substituent in the chromenone moiety (R_1 = OCH_3), which might reduce the H-bond donor ability of the adjacent OH group, which is responsible for the formation of a stable H-bond with the hydroxyl-substituted side chain of residue S249, as shown by the docking analysis of compound **4** in the LDH active site (Fig. 3).

In conclusion, this is the first report of flavonoid glycosides and phenylpropanoids displaying a certain degree of *h*LDH5-inhibitory activities and these results may be useful for the perspective development of new anticancer agents starting from these natural products.

3. Experimental

3.1. General

A Perkin-Elmer 241 polarimeter equipped with a sodium lamp (589 nm) and a 1 dm microcell was used to measure optical rotations. UV spectra were registered on a Perkin-Elmer-Lambda spectrophotometer. NMR experiments were recorded on a Bruker DRX-600 and Bruker Avance 250 spectrometer at 300 K, acquiring the spectra in methanol-d_4. Standard pulse sequences and phase cycling were used for TOCSY, HSQC, DQF-COSY, HMBC, and ROESY experiments. NMR data were processed using XWIN-NMR software. HRESIMS were obtained in the positive ion mode on a Q-TOF premier spectrometer equipped with a nanospray ion source (Waters Milford,

MA, USA). ESIMS were obtained from an LCQ Advantage ThermoFinnigan spectrometer (ThermoFinnigan, USA). Sephadex LH-20 or silica gel 60 (Merck, 60-230 mesh) was used for column chromatography. HPLC analyses were performed over Shimadzu LC-8A series pumping system equipped with a Shimadzu RID-10A refractive index detector and Shimadzu injector on a C_{18} μ-Bondapak column (30 cm x 7.8 mm, 10 μm Waters, flow rate 2.0 ml min^{-1}) using mixture MeOH-H_2O as eluents. TLC separations were carried out using silica gel 60 F_{254} (0.20 mm thickness) plates (Merck) with *n*-BuOH-CH_3COOH-H_2O (60:15:25) as eluent and cerium sulphate as spray reagent. GC analyses were performed using a Dani GC 1000 instrument on a L-CP-Chirasil-Val column (0.32 mm x 25 m) working with the following temperature programme: 100 °C for 1 min, ramp of 5 °C/min up to 180 °C; injector and detector temperature 200 °C; carrier gas N_2 (2 mL/min); detector dual FID; split ratio 1:30; injection 5 μL.

3.2. Plant material

P. kurdica aerial parts were collected in Al-Yadoudeh, Jordan, during April 2009 and were identified by one of the authors (A. Bader). A voucher specimen (number Jo-It 2009/1) is deposited in herbarium of the laboratory of Pharmacognosy, Umm Al-Qura University, Makkah, Saudi Arabia.

3.3. Extraction and isolation

The powdered dried aerial parts of *P. kurdica* (400 g) were extracted with solvents of increasing polarity, *n*-hexane, $CHCl_3$, $CHCl_3$-MeOH (9:1), and MeOH (3 × 2 L), to give 4.7, 5.1, 8.1, and 23 g of the respective residue. Part of the $CHCl_3$-MeOH extract (3.0 g) was separated by CC using Sephadex LH-20 (2.5 x 100 cm) with MeOH as eluent at flow rate 0.8 mL/min. TLC results led to fractions being pooled into six groups (A_1-F_1). Groups B_1 (240 mg, 590-650 mL) and E_1 (61 mg,

1170-1260 mL) were chromatographed by RP-HPLC with MeOH-H_2O (4.5:5.5) to give pure compound **3** (4.7 mg, t_R = 17 min), from group B_1 and pure compounds **5** (5.4 mg, t_R = 35 min) and **9** (3.0 mg, t_R = 23 min), from group E_1, respectively. The MeOH extract was partitioned between *n*-BuOH and H_2O to give 10.0 g of a *n*-BuOH residue. Sephadex LH-20 column chromatography (5 x 100 cm) was employed to separate the *n*-BuOH soluble fraction (2.5 g); MeOH, at flow rate of 0.8 mL/min, was used as eluent, and eleven groups (A_2-K_2) were collected. Groups C_2 (385.8 mg, 440-500 mL), D_2 (383.9 mg, 510-600 mL), E_2 (179.3 mg, 610-720 mL), F_2 (101.2 mg, 730-760 mL), and G_2 (78.1 mg, 770-930 mL) were purified by RP-HPLC with MeOH-H_2O (2:3) as eluent to yield compound **11** (2.5 mg, t_R = 35 min), from group C_2, **12** (3.0 mg, t_R = 6 min) and **8** (3.9 mg, t_R = 11 min), from group D_2, **8** (8.5 mg, t_R = 11 min), **13** (10.2 mg, t_R = 12 min), **2** (4.8 mg, t_R = 27 min), and **1** (3.9 mg, t_R = 29 min), from group E_2, **13** (27.0 mg, t_R = 12 min), from group F_2, and **6** (5.2 mg, t_R = 16 min), **10** (10.5 mg, t_R = 24 min), **5** (3.2 mg, t_R = 30 min), **7** (3.5 mg, t_R = 36 min), from group G_2, respectively. Group I_2 (100.0 mg, 1050-1180 mL) was purified by RP-HPLC eluting with MeOH-H_2O (4.5:5.5) to give compound **4** (5.5 mg, t_R = 15 min). Group J_2 (75.8 mg, 1190-1300 mL) was subjected to silica gel column chromatography eluting with $CHCl_3$-MeOH 95:5 followed by increasing concentrations of MeOH in $CHCl_3$ (575 mL $CHCl_3$-MeOH 95:5, 580-620 mL $CHCl_3$-MeOH 93:7, 625-730 mL $CHCl_3$-MeOH 9:1, 735-980 mL $CHCl_3$-MeOH 7:3, 985-1225 mL $CHCl_3$-MeOH 1:1) to obtain pure compound **14** (7.7 mg, 1050-1225 mL).

*3.3.1. Compound **1***

Yellow amorphous powder; $[\alpha]_D^{25}$ -47 (*c* 0.1, MeOH); UV (MeOH) λ_{max} (log ε) 277 (4.01), 340 (3.85) nm; ^1H and ^{13}C NMR, see Table 1; ESIMS *m/z* 677 $[M+Na]^+$, 353 $[M+Na–162–162]^+$, 653 $[M–H]^–$, 491 $[M–H–162]^–$, 329 $[M–H–162–162]^–$; HRESIMS *m/z* 653.1725 $[M–H]^–$ (calcd for $C_{29}H_{33}O_{17}$ 653.1718).

*3.3.2. Compound **2***

Yellow amorphous powder; $[\alpha]_D^{25}$+26 (*c* 0.05, MeOH); UV (MeOH) λ_{max} (log ε) 277 (3.95), 332 (3.77) nm; ^{1}H and ^{13}C NMR, see Table 1; ESIMS *m/z* 647 $[M+Na]^+$, 623 $[M–H]^–$, 299 $[M–H–162–162]^–$; HRESIMS *m/z* 623.1608 $[M–H]^–$ (calcd for $C_{28}H_{31}O_{16}$ 623.1612).

3.3.3. Compound ***3***

Brown amorphous powder; $[\alpha]_D^{25}$132 (*c* 0.05, MeOH); UV (MeOH) λ_{max} (log ε) 230sh (3.66), 288sh (3.84), 330 (4.00) nm; ^{1}H NMR δ 1.10 (3H, d, *J* = 6.5 Hz, H-6$_{rha}$), 2.86 (2H, m, H$_2$-7$_{agl}$), 3.41 (1H, dd, *J* = 9.0, 7.8 Hz, H-2$_{glc}$), 3.42 (1H, dd, *J* = 9.0, 3.0 Hz, H-3$_{rha}$), 3.48 (1H, dd, *J* = 12.0, 4.5 Hz, H-6b$_{glc}$), 3.53 (2H, br s, H$_2$-5$_{apiI}$), 3.57 (2H, br s, H$_2$-5$_{apiII}$), 3.59 (1H, t, *J* = 9.0 Hz, H-4$_{rha}$), 3.62 (1H, m, H-5$_{rha}$), 3.72 (1H, m, H-5$_{glc}$), 3.75 (1H, d, *J* = 10.0 Hz, H-4b$_{apiI}$), 3.77 (1H, m, H-8b$_{agl}$), 3.78 (1H, dd, *J* = 12.0, 3.0 Hz, H-6a$_{glc}$), 3.79 (3H, s, OMe$_{agl}$), 3.81 (1H, t, *J* = 9.0 Hz, H-3$_{glc}$), 3.86 (1H, br s , H-2$_{apiI}$), 3.91 (1H, d, *J* = 10.0 Hz, H-4b$_{apiII}$), 3.92 (1H, d, *J* = 10.0 Hz, H-4a$_{apiI}$), 3.96 (3H, s, OMe$_{fer}$), 3.96 (1H, br s , H-2$_{apiII}$), 4.05 (1H, d, *J* = 10.0 Hz, H-4a$_{apiII}$), 4.06 (1H, m, H-8a$_{agl}$), 4.07 (1H, dd, *J* = 3.0, 1.8 Hz, H-2$_{rha}$), 4.36 (1H, d, *J* = 7.8 Hz, H-1$_{glc}$), 4.88 (1H, d, *J* = 3.0 Hz, H-1$_{apiII}$), 4.90 (1H, t, *J* = 9.0 Hz, H-4$_{glc}$), 5.15 (1H, d, *J* = 3.0 Hz, H-1$_{apiI}$), 5.17 (1H, d, *J* = 1.8 Hz, H-1$_{rha}$), 6.39 (1H, d, *J* = 16.0 Hz, H-α$_{fer}$), 6.70 (1H, d, *J* = 2.0 Hz, H-2$_{agl}$), 6.72 (1H, dd, *J* = 8.0, 2.0 Hz, H-6$_{agl}$), 6.80 (1H, d, *J* = 8.0 Hz, H-5$_{fer}$), 6.87 (1H, d, *J* = 8.0 Hz, H-5$_{agl}$), 7.09 (1H, dd, *J* = 8.0, 2.0 Hz, H-6$_{fer}$), 7.21 (1H, d, *J* = 2.0 Hz, H-2$_{fer}$), 7.65 (1H, d, *J* = 16.0 Hz, H-β$_{fer}$); ^{13}C NMR δ 18.3 (C-6$_{rha}$), 36.7 (C-7$_{agl}$), 56.1 (OMe$_{agl}$), 56.5 (OMe$_{fer}$), 65.2 (C-5$_{apiII}$), 65.6 (C-5$_{apiI}$), 68.4 (C-6$_{glc}$), 70.4 (C-5$_{rha}$), 70.5 (C-4$_{glc}$), 72.0 (C-8$_{agl}$), 72.3 (C-2$_{rha}$), 72.4 (C-3$_{rha}$), 74.8 (C-5$_{glc}$), 74.9 (C-4$_{apiI}$ and C-4$_{apiII}$), 76.0 (C-2$_{glc}$), 77.9 (C-2$_{apiI}$), 78.0 (C-2$_{apiII}$), 80.3 (C-4$_{rha}$), 80.4 (C-3$_{apiI}$), 80.5 (C-3$_{apiII}$), 81.5 (C-3$_{glc}$), 102.9 (C-1$_{rha}$), 104.2 (C-1$_{glc}$), 111.0 (C-1$_{apiII}$), 111.7 (C-2$_{fer}$), 111.8 (C-1$_{apiI}$), 113.5 (C-5$_{agl}$), 115.0 (C-α$_{fer}$), 116.0 (C-2$_{agl}$), 116.6 (C-5$_{fer}$), 122.4 (C-6$_{agl}$), 124.2 (C-6$_{fer}$), 128.0 (C-1$_{fer}$), 130.5 (C-1$_{agl}$), 145.0 (C-4$_{agl}$), 146.0 (C-4$_{fer}$), 148.0 (C-β$_{fer}$), 148.1 (C-3$_{agl}$), 150.5 (C-3$_{fer}$), 168.1 (COO); ESIMS *m/z* 939

$[M+Na]^+$, 807 $[M+Na–132]^+$, 675 $[M+Na–132–132]^+$, 661 $[M+Na–132–146]^+$, 915 $[M–H]^–$; HRESIMS *m/z* 915.3120 $[M–H]^–$ (calcd for $C_{41}H_{55}O_{23}$ 915.3134).

*3.4. Acid hydrolysis of compounds **1-3***

Acid hydrolysis of compounds **1-3** was carried out as reported before in our previous paper (Dal Piaz et al., 2013). D-glucose, L-rhamnose, and D-apiose were identified as sugar moieties by comparison with retention times of authentic samples.

3.5. LDH assays

The LDH inhibition properties of extracts and isolated compounds were evaluated against purified human lactate dehydrogenase isoform 1 and 5 (Lee Biosolution, Inc.). The "forward" direction (pyruvate → lactate) of the lactate dehydrogenase reaction was conducted, and the kinetic parameters were measured by fluorescence (emission wavelength at 460 nm, excitation wavelength at 340 nm) to monitor the amount of consumed NADH (for IC_{50} measurements), or the rate of conversion of NADH to NAD^+ (for K_i measurements). Assays were carried out in wells containing 200 µL of a reagents solution dissolved in 100 mM phosphate buffer (pH = 7.4). For extracts, 100 µL of each resuspended sample (0.8 mg/mL) in DMSO (the concentration of DMSO did not exceed 4% during the measurements) were three-fold serially diluted, whereas, for the IC_{50} calculations of the compounds, seven different concentrations (in duplicate for each concentration) of the isolated compounds were used to produce the concentration–response curve. Both extracts and isolated compounds were tested in the presence of 200 µM pyruvate and 40 µM NADH. Any background fluorescence likelihood of the tested samples, or NADH fluorescence quenching, was subtracted. As well as the sample test wells, maximum and minimum controls were also included in each plate. After 15 min of incubation, the final measurements were carried out by using a Victor X3

Microplates Reader (PerkinElmer®). IC_{50} values were produced using GraphPad Prism software (GraphPad – USA). We followed an analog procedure previously reported by us (Granchi et al., 2013), verifying the linearity with respect to time over 15 minutes. In the kinetics experiments in competition with NADH, compound **4** was tested together with scalar NADH concentrations. The compound was added (concentration range = 25–100 μM) to a reaction mixture containing 1.4 mM pyruvate, scalar concentrations of NADH (concentration range = 10–150 μM), and potassium phosphate buffer 100 mM (pH = 7.4). Finally, LDH solution was added (0.015 U/mL) and the enzyme activity was measured by evaluating the NADH fluorescence decrease using a Victor X3 Microplates Reader (PerkinElmer®). A non-linear regression analysis was used for analyzing the experimental data, using a second order polynomial regression analysis, and by applying the mixed-model inhibition fit (Copeland, 2000). The kinetic experiments in competition with PYR were carried out similarly as described above, by using 150 μM NADH, and scalar concentrations of PYR (concentration range = 40–500 μM).

3.6. Molecular modeling studies

The hLDH5 crystal structure (pdb code 4M49) (Fauber et al., 2013) was taken from the Protein Data Bank (Berman et al., 2000). Hydrogen atoms were added to the protein complexed with its reference inhibitor and then it was minimized using AMBER11 software (Case et al., 2010) and parm03 force field at 300 K. The complex was arranged in a parallelepiped water box, and it was solvated with a 10 Å water cap of an explicit solvent model for water (TIP3P). Chlorine ions were added as counterions for neutralizing the system. Two steps of minimization were then carried out; in the first stage, we minimized the positions of the water molecules, keeping the protein fixed with a position restraint of 500 kcal/mol Å (Fauber et al., 2013). In the second stage, the entire system was minimized through 5000 steps of steepest descent followed by conjugate gradient (CG) until a convergence of 0.05 kcal/Å mol. Maestro software (Maestro, 2009) was used for building the ligand

and Macromodel (Macromodel, 2009) was used for minimizing it in a water environment by using the CG method until a convergence value of 0.05 kcal/Å mol, using the MMFFs force field and a distance-dependent dielectric constant of 1.0. Docking evaluation was carried out through the GOLD 5.1 program (Verdonk et al., 2003). The binding site for the docking evaluation was defined in such a manner that it was constituted by all residues within 10 Å of the reference ligand and NADH co-factor in the X-ray crystal structure (pdb code 4M49). The possibility for the ligand to flip ring corners was activated whereas the "allow early termination" command was deactivated. All the other GOLD default parameters were used, and the ligand was submitted to 100 genetic algorithm runs by applying the PLP fitness function. The best scored conformation was then subjected to molecular dynamic simulations. AMBER11 was used for performing the simulations and the input preparation and minimization stages were the same reported above. Molecular dynamics trajectory was then run using the minimized structure as the input, and periodic boundary conditions and particle mesh Ewald electrostatics (Essmann et al., 1995) were used in the simulation. SHAKE was employed to keep all bonds involving hydrogen atoms rigid. The time step of the simulations was 2.0 fs with a cutoff of 12 Å for the non-bonded interaction. The General Amber Force Field (GAFF) parameters were assigned to the ligand. The partial charges were determined using the AM1-BCC method of the Antechamber suite of AMBER 11.

Acknowledgements

C. Granchi and F. Minutolo gratefully acknowledge the NIH (R01GM098453) for funding.

References

Agrawal, P. K., 1989. Carbon-13 NMR of Flavonoids. Elsevier. Amsterdam.

Al-Eisawi, D. M., 1998. Field Guide to Wild Flowers of Jordan and Neighboring Countries. The National Library. Amman, 117.

Berman, H. M., Westbrook, J., Feng, Z., Gilliland, G., Bhat, T. N., Weissig, H., Shindyalov, I. N., Bourne, P. E., 2000. The Protein Data Bank. Nucleic Acids Res. 28, 235-242.

Calis, I., Kirmizibekmez, H., 2004. Glycosides from *Phlomis lunariifolia*. Phytochemistry 65, 2619-2625.

Case, D. A., Darden, T. A., Cheatham, T. E. III, Simmerling, C. L., Wang, J., Duke, R. E., Luo, R., Walker, R. C., Zhang, W., Merz, K. M., Roberts, B., Wang, B., Hayik, S., Roitberg, A., Seabra, G., Kolossváry, I., Wong, K. F., Paesani, F., Vanicek, J., Liu, J., Wu, X., Brozell, S. R., Steinbrecher, T., Gohlke, H., Cai, Q., Ye, X., Wang, J., Hsieh, M.-J., Cui, G., Roe, D. R., Mathews, D. H., Seetin, M. G., Sagui, C., Babin, V., Luchko, T., Gusarov, S., Kovalenko, A., Kollman, P. A., 2010. AMBER. Version 11; in University of California: San Francisco, CA.

Copeland, R. A., 2000. Enzymes: a practical introduction to structure, mechanism, and data analysis. 2nd ed. Wiley. New York, xvi, 397.

Dal Piaz, F., Vassallo, A., Lepore, L., Tosco, A., Bader, A., De Tommasi N., 2009 J. Sesterpenes as tubulin tyrosine ligase inhibitors. First insight of structure-activity relationships and discovery of new lead. J. Med. Chem. 52, 3814-3828.

Dal Piaz, F., Vassallo, A., Temraz, A., Cotugno, R., Belisario, M. A., Bifulco, G., Chini, M. G., Pisano, C., De Tommasi, N., Braca, A., 2013. A chemical-biological study reveals C_9-type iridoids as novel heat shock protein 90 (Hsp90) inhibitors. J. Med. Chem. 56, 1583-1595.

Endo, K., Takahashi, K., Abe, Y., Hikino, H., 1982. Structure of forsythoside B, an antibacterial principle of *Forsythia koreana* stems. Heterocycles 19, 261-271.

Essmann, U., Perera, L., Berkowitz, M. L., Darden, T., Lee, H., Pedersen, L. G., 1995. A smooth particle mesh Ewald method. J. Chem. Phys. 103, 8577-8593.

Fauber, B. P., Dragovich, P. S., Chen, J., Corson, L. B., Ding, C. Z., Eigenbrot, C., Giannetti, A. M., Hunsaker, T., Labadie, S., Liu, Y., Malek, S., Peterson, D., Pitts, K., Sideris, S., Ultsch, M., VanderPorten, E., Wang, J., Wei, B., Yen, I., Yue, Q., 2013. Identification of 2-amino-5-aryl-pyrazines as inhibitors of human lactate dehydrogenase. Bioorg. Med. Chem. Lett. 23, 5533-5539.

Fiume, L., Manerba, M., Vettraino, M., Di Stefano, G., 2014. Inhibition of lactate dehydrogenase activity as an approach to cancer therapy. Future Med. Chem. 6, 429-445.

Granchi, C., Calvaresi, E. C., Tuccinardi, T., Paterni, I., Macchia, M., Martinelli, A., Hergenrother, P. J., Minutolo, F., 2013. Assessing the differential action on cancer cells of LDH-A inhibitors based on the *N*-hydroxyindole-2-carboxylate (NHI) and malonic (Mal) scaffolds. Org. Biomol. Chem. 11, 6588-6596.

Granchi, C., Minutolo, F., 2012. Anticancer agents that counteract tumor glycolysis. ChemMedChem 7, 1318-1350.

Granchi, C., Paterni, I., Rani, R., Minutolo, F., 2013. Small-molecule inhibitors of human LDH5. Future Med. Chem. 5, 1967–1991.

Imperato, F., Nazzaro, R., 1996. Luteolin 7-*O*-sophoroside from *Pteris cretica*. Phytochemistry 41, 337-338.

Iwai, K., Kishimoto, N., Kakino, Y., Mochida, K., Fujita, T., 2004. In vitro antioxidative effects and tyrosinase inhibitory activities of seven hydroxycinnamoyl derivatives in green coffee beans. J. Agric. Food Chem. 52, 4893-4898.

Kirmizibekmez, H., Montoro, P., Piacente, S., Pizza, C., Dönmez A., Çalıs I., 2005. Identification by HPLC-PDA-MS and quantification by HPLC-PDA of phenylethanoid glycosides of five *Phlomis* species. Phytochem. Anal. 16, 1-6.

Li, M-X., Shang, X-F., Jia, Z-P., Zhang, R-X., 2010. Phytochemical and biological studies of plants from the genus *Phlomis*. Chem. Biodivers. 7, 283-301.

Limem-Ben Amor, I., Boubaker, J., Ben Sgaier, M., Skandrani, I., Bhouri, W., Neffati, A., Kilani, S., Bouhlel, I., Ghedira, K., Chekir-Ghedira, L., 2009. Phytochemistry and biological activities of *Phlomis* species. J. Ethnopharmacol. 125, 183-202.

Liu, Y., Wagner, H., Bauer, R., 1998. Phenylpropanoids and flavonoid glycosides from *Lysionotus pauciflorus*. Phytochemistry 48, 339-343.

Ma, C. Y., Zhu, K. X., Yang, D. M., Yang, J. S., Ju, D. Q., 1991. Chemical constituents of *Veronica linariifolia* Pall. Ex Link. Yaoxue Xuebao 26, 203-208.

Macromodel, 2009. Version 9.7; in Schrödinger Inc: Portland, OR.

Maestro, 2009. Version 9.0; in Schrödinger Inc: Portland, OR.

Malafronte, N., Vassallo, A., Dal Piaz, F., Bader, A., Braca, A., De Tommasi N., 2012. Biflavonoids from *Daphne linearifolia* Hart. Phytochemistry Lett. 5, 621-625.

Manerba, M., Vettraino, M., Fiume, L., Di Stefano, G., Sartini, A., Giacomini, E., Buonfiglio, R., Roberti, M., Recanatini, M., 2012. Galloflavin (CAS 568-80-9): a novel inhibitor of lactate dehydrogenase. ChemMedChem 7, 311-317.

Martinez, V., Barbera, O., Sanchez-Parareda, J., Alberto Marco, J., 1987. Phenolic and acetylenic metabolites from *Artemisia assoana*. Phytochemistry 26, 2619-2624.

Merfort, I., 1988. Acylated and other flavonoid glycosides from *Arnica chamissonis*. Phytochemistry 27, 3281-3284.

Merfort, I., Wendish, D., 1987. Flavonoid glycosides from *Arnica montana* and *Arnica chamissonis*. Planta Med. 53, 434-437.

Miyase, T., Koizumi, A., Ueno, A., Noro, T., Kuronayagi, M., Fukushima, S., Akiyama, Y., Takemoto, T., 1982. Studies on the acyl glycosides from *Leucoseptrum japonicum* (Miq.) Chem. Pharm. Bull. 30, 2732-2737.

Sakushima, A., Coskun, M., Maoka, T., 1995. Hydroxybenzoic acid from *Boreava orientalis*. Phytochemistry 40, 257-261.

Tuccinardi, T., 2009. Docking-based virtual screening: recent developments. Comb. Chem. High Throughput Screen. 12, 303-314.

Verdonk, M. L., Cole, J. C., Hartshorn, M. J., Murray, C. W., Taylor, R. D., 2003. Improved protein-ligand docking using GOLD. Proteins 52, 609-623.

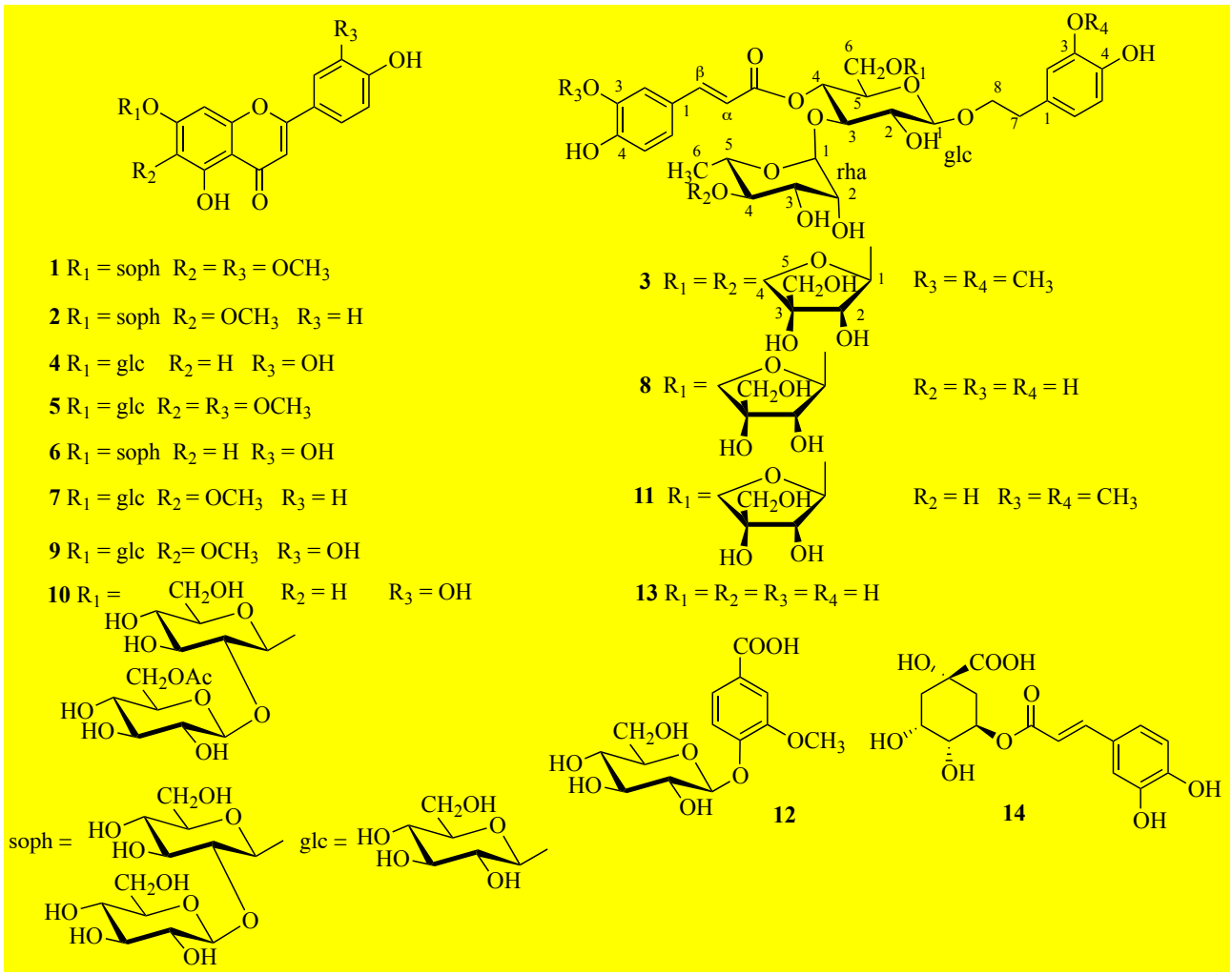

Fig. 1. Structures of compounds **1-14** isolated from *P. kurdica*

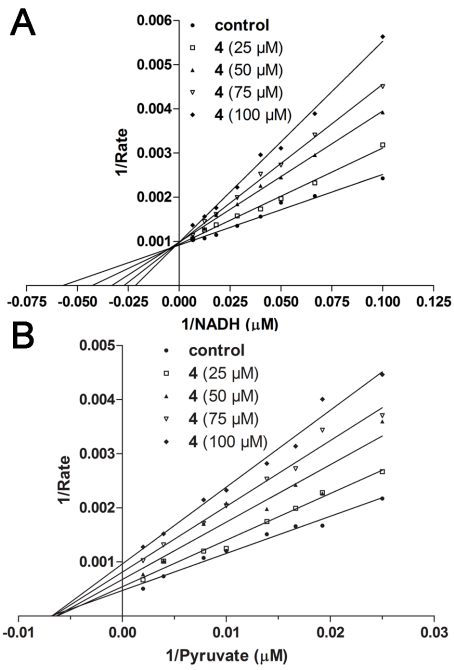

Fig. 2. Lineweaver-Burk plots determined for compound **4**: competition experiments with NADH (A) and pyruvate (B).

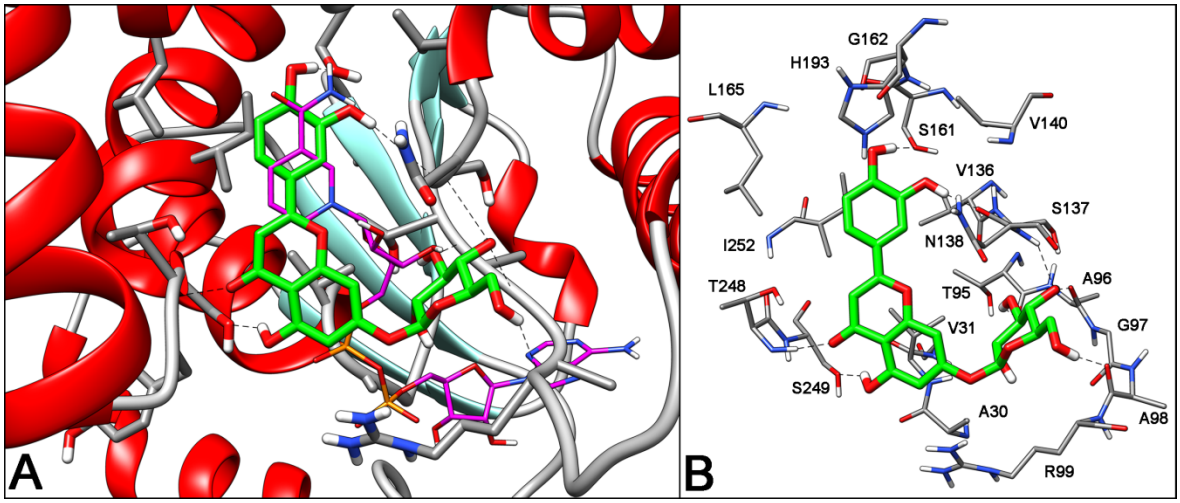

Fig. 3. Suggested binding mode of compound **4** into *h*LDH5. A) Putative binding pose of the ligand (green) in the binding site, NADH (magenta) is reported as a reference disposition; B) view of the most relevant ligand-receptor interactions.

Table 1

^{1}H and ^{13}C NMR data of compounds **1-2**. [a]

	1		**2**	
position	δ_H	δ_C	δ_H	δ_C
2		167.1		167.4
3	6.78 s	103.5	6.71 s	103.0
4		183.6		184.0
5		154.3		154.1
6		134.2		134.4
7		158.0		157.0
8	7.04 s	94.6	6.98 s	95.0
9		157.0		157.2
10		107.3		107.1
1'		123.8		123.2
2'	7.58 d (2.0)	110.4	7.91 d (8.5)	129.4
3'		149.3	6.95 d (8.5)	117.0
4'		152.5		163.8
5'	6.96 d (8.0)	116.4	6.95 d (8.5)	117.0
6'	7.60 dd (8.0, 2.0)	121.8	7.91 d (8.5)	129.4
6-OCH_3	3.93 s	60.9	3.89 s	61.0
3'-OCH_3	4.00 s	56.2		
Glc I 1	5.38 d (7.5)	99.4	5.40 d (7.8)	100.0
2	3.90 dd (9.0, 7.5)	82.0	3.88 dd (9.5, 7.8)	82.0
3	3.76 t (9.0)	77.4	3.76 t (9.5)	77.0
4	3.48 t (9.0)	70.6	3.54 t (9.5)	70.0
5	3.62 m	77.8	3.61 m	78.0
6a	3.98 dd (12.0, 3.0)	61.9	3.96 dd (12.0, 2.5)	62.5
6b	3.74 dd (12.0, 4.5)		3.73 dd (12.0, 4.5)	
Glc II 1	4.85 d (7.5)	104.0	4.79 d (7.5)	104.3
2	3.25 dd (9.0, 7.5)	75.2	3.26 dd (9.0, 7.5)	75.8
3	3.42 t (9.0)	77.2	3.40 t (9.0)	78.0
4	3.40 t (9.0)	70.6	3.48 t (9.0)	70.0
5	3.31 m	77.1	3.30 m	77.8
6a	3.62 dd (12.0, 3.0)	61.3	3.66 dd (12.0, 3.0)	62.0
6b	3.48 dd (12.0, 4.5)		3.46 dd (12.0, 4.5)	

[a] Spectra were run in methanol-d_4 at 600 MHz (^{1}H) and 150 MHz (^{13}C). *J* values are in parentheses and reported in Hz; chemical shifts are given in ppm; assignments were confirmed by COSY, 1D-TOCSY, HSQC, and HMBC experiments.

Table 2

*h*LDH5 inhibition potencies.

Extract	***h*LDH5**[a] **(IC_{50}, mg/mL)**
RCM[b]	0.49 ± 0.08
RM[c]	0.59 ± 0.26
RB[d]	0.28 ± 0.03
Compound	***h*LDH5**[a] **(IC_{50}, µM)**
1	259.9 ± 9.8
2	> 500
3	> 500
4	139.2 ± 3.1
5	153.0 ± 11.5
6	163.2 ± 7.8
7	209.8 ± 44.3
8	224.6 ± 19.7
9	298.4 ± 45.1
10	445.0 ± 46.5
11	> 500
12	> 500
13	> 500
14	> 500
Galloflavin	103.6 ± 22.6 (201)[e]

[a] Values are reported as the means ± SD of three or more independent experiments.
[b] RCM = chloroform-MeOH (9:1) extract.
[c] RM = methanol extract.
[d] RB = *n*-butanol extract.
[e] Value reported in ref 22.